

Mars Balloon Flight Test Results

Jeffery L. Hall¹, Michael T. Pauken², Viktor V. Kerzhanovich³, Gerald J. Walsh⁴ and Eric A. Kulczycki⁵
Jet Propulsion Laboratory, California Institute of Technology, Pasadena, CA, 91109

Debora Fairbrother⁶ and Chris Shreves⁷
Wallops Flight Facility, Goddard Space Flight Center, Wallops Is, VA

and

Tim Lachenmeier⁸
Near Space Corporation, Tillamook, OR, 97141

This paper describes a set of four Earth atmosphere flight test experiments on prototype helium superpressure balloons designed for Mars. Three of the experiments explored the problem of aerial deployment and inflation, using the cold, low density environment of the Earth's stratosphere at an altitude of 30-32 km as a proxy for the Martian atmosphere. Auxiliary carrier balloons were used in three of these test flights to lift the Mars balloon prototype and its supporting system from the ground to the stratosphere where the experiment was conducted. In each case, deployment and helium inflation was initiated after starting a parachute descent of the payload at 5 Pa dynamic pressure, thereby mimicking the conditions expected at Mars after atmospheric entry and high speed parachute deceleration. Upward and downward looking video cameras provided real time images from the flights, with additional data provided by onboard temperature, pressure and GPS sensors. One test of a 660 m³ pumpkin balloon was highly successful, achieving deployment, inflation and separation of the balloon from the flight train at the end of inflation; however, some damage was incurred on the balloon during this process. Two flight tests of 12 m diameter spherical Mylar balloons were not successful, although some lessons were learned based on the failure analyses. The final flight experiment consisted of a ground-launched 12 m diameter spherical Mylar balloon that ascended to the designed 30.3 km altitude and successfully floated for 9.5 hours through full noontime daylight and into darkness, after which the telemetry system ran out of electrical power and tracking was lost. The altitude excursions for this last flight were ± 75 m peak to peak, indicating that the balloon was essentially leak free and functioning correctly. This provides substantial confidence that this balloon design will fly for days or weeks at Mars if it can be deployed and inflated without damage.

I. Introduction

This paper describes a set of four new Mars superpressure balloon flight experiments that are the latest in a series of such tests conducted by a joint JPL, NASA-Wallops and Near Space Corporation team. These experiments have focused on the technology of aerial deployment and inflation for helium-filled balloons. During this process, the Mars balloon transitions from a compact, folded structure inside the carrier spacecraft to a fully deployed and inflated balloon floating in the atmosphere. The technical challenge of this process is that a balloon must be very

¹ Senior Engineer, Mobility & Robotic Systems, 4800 Oak Grove Dr., M/S 82-105, Senior Member AIAA.

² Senior Engineer, Thermal & Cryogenic Engineering, 4800 Oak Grove Dr., M/S 125-123, Member AIAA.

³ Principal Member of the Technical Staff, Mobility & Robotic Systems, 4800 Oak Grove Dr., M/S 198-219.

⁴ Senior Engineer, Exciter & RF/Millimeter-Wave Instruments, 4800 Oak Grove Dr., M/S 238-737.

⁵ Staff Engineer, Mobility & Robotic Systems, 4800 Oak Grove Dr., M/S 82-105

⁶ Balloon Program Chief Technologist, Balloon Program Office, MS Code 820, Associate Fellow AIAA.

⁷ Aerospace Engineer, Mechanical Systems Branch.

⁸ President, P.O. Box 909, Senior Member AIAA.

lightweight to float in the thin Martian atmosphere, but the resultant structural fragility makes it difficult to endure the deployment and inflation process without suffering damage. Previous papers (Refs 1 and 2) have documented earlier results from analysis, laboratory experiments and Earth atmosphere flight experiments that demonstrated progress but no comprehensive technical solution. Many flight experiments with full scale prototype Mars balloons have been conducted at a 30+ km altitude in the Earth’s stratosphere to best replicate the low density ($\sim 0.02 \text{ kg/m}^3$) and low temperature ($\sim 226 \text{ K}$) conditions found at Mars. The accumulated results have emphasized the importance of using large parachutes to provide low dynamic pressures ($\sim 5 \text{ Pa}$) on the inflating balloon and using force limiting elements (e.g., ripstitch) in the flight train to prevent balloon destruction from excessive deployment structural loads. Other important system design features will be discussed in later sections.

For the work reported here, the team has continued the strategy of parallel development of both spherical thin-film and pumpkin balloon options for the Mars balloon. The spherical balloon used here is a 12 m diameter, 12.7 μm thin-film Mylar design with adhesively joined gores and reinforced end caps. The pumpkin balloon is a 660 m^3 design with Zylon tendons and 15 μm co-extruded polyethylene film. The advantage of the spherical balloon is that it is lighter and simpler to construct. The advantage of the pumpkin balloon is that the tendons provide significant strength for tolerating the transient loads during deployment and inflation. Of the four experiments reported here, three flew spherical Mylar balloons and one with the pumpkin balloon. Properties of both balloons are summarized in Table 1. The spherical balloons were fabricated by Near Space Corporation, and the pumpkin balloon was fabricated by Aerostar International.

II. Design and Test Methodology

Stratospheric flight testing is required to evaluate the performance of the Mars balloon designs at the system level. The Earth’s stratosphere provides the best proxy environment for Mars because of the importance of matching the atmospheric density for the aerodynamic behavior of the system. Such testing is actually more severe than what would be experienced at Mars because the higher Earth gravitational acceleration ($9.8 \text{ vs } 3.7 \text{ m/s}^2$) results in a much higher balloon deployment speed and attendant deployment shock load. These flight experiments use a carrier balloon to lift the Mars prototype balloon and flight train from the ground to the stratospheric altitude. The flight test sequence of events is illustrated in Fig. 1. The aerial deployment and inflation experiment begins when the flight train is detached from the carrier balloon and commences parachute descent at a dynamic pressure equivalent to that which will be experienced at Mars (Step 4 in Fig. 1). Balloon inflation with helium gas occurs over a short period (150 s in this example) and completes at Step 8. Note that at Step 7 a pyrotechnical cable cutter is used to cut one of the four parachute suspension lines, which in turn engages a secondary suspension line that is 2 meters longer. This event makes the parachute geometrically asymmetrical and causes a lateral drift in the descent velocity vector. This lateral motion ensures that the parachute does not fall on top of the Mars balloon when the parachute-balloon separation event occurs in Step 8. The helium tanks are jettisoned simultaneously with the parachute. The Mars balloon is a free-floating vehicle at this point and will rise to its design altitude and stabilize there (Step 9).

The current set of four flight experiments were all launched from the Near Space Corporation facility in Ocean View, Hawaii. Table 2 lists the flight dates and other basic information. Figure 2 shows the arrangement of the flight train prior to launch for aerial deployment test STRA-15. The blue Styrofoam box-like structure in the foreground contains the rolled up prototype Mars balloon, the helium tanks and inflation plumbing, avionics for receiving radio

Table 1: Balloon Design Parameters

	Spherical	Pumpkin
Volume	900 m^3	660 m^3
Polar Height	12.0 m	7.5 m
Equatorial Diameter	12.0 m	12.2 m
Film Material	Polyester	Polyethylene
Film Thickness	12.7 μm	15.2 μm
Gores	28	56
Tendon Material	N/A	Zylon, 8000 denier
Total Mass (incl. fittings)	9.9 kg	10.5 kg

commands from the ground, a radiosonde, and an upwards-looking TV camera, transmitter electronics and wheel antenna. Laid out on the carpet behind that is the cross parachute with an orange canopy, and finally the zero-pressure polyethylene carrier balloon that is being inflated. The blue payload box was light enough ($<65 \text{ kg}$) that a hand-carried launch procedure was used to ensure that it and the other the flight train components did not drag across the ground when the carrier balloon was launched and began to ascend. This flight train arrangement was essentially the same for tests STRA-13 and STRA-14 also.

Fig. 3 is a schematic diagram that shows the flight train arrangement at Step 5 (from Fig. 1) for the three aerial deployment tests, namely during parachute descent with a deployed but not yet inflated Mars balloon. The three main

Table 2: Summary of Flight Test Experiment Parameters

Designation	STRA-13	STRA-14	STRA-15	GRND-1
Balloon Type	Sphere	Pumpkin	Sphere	Sphere
Balloon Size	900 m ³	660 m ³	900 m ³	900 m ³
Test Date	6/27/07	6/30/07	6/14/08	6/11/08
Test Objective	Aerial Deployment	Aerial Deployment	Aerial Deployment	Ground Launch
Total Mass Under Carrier Balloon (kg)	82.6	79.3	84.7	N/A
Parachute Diameter (m)	21	21	21	N/A
Helium Mass in Tanks (kg)	2.4	2.0	2.4	N/A
Design Carrier Balloon Float Altitude (km)	30.8	28.9	30.2	30.1
Design Mars Balloon Deploy Altitude (km)	32.0	31.0	30.0	N/A

components (payload module, Mars balloon, parachute) are connected with Kevlar rope and carabiners to a number of secondary components to form the overall flight train. Three of the four ripstitch elements are used to mitigate deployment shock loads caused by acceleration of flight train components: L1 for the payload module, U3 for the upper cable cutter, and U2 for the upper TV box containing the camera, transmitter and antenna. The fourth ripstitch, U1, is designed to rip at the moment of balloon deployment and add 50 m of length between the balloon and parachute. We use a ripstitch for this purpose to avoid adding 50 m of flight train length on the ground and the increased difficulty of launching such a long experimental package. This long separation distance between the parachute and the balloon reduces oscillations in the parachute from vortices shed from the balloon. All ripstitches were constructed from MIL-W-4088K Type IV webbing and Nylon thread. Black marks were made at regular intervals on the ripstitch to assist with the post-flight video determination of how much ripping actually occurred.

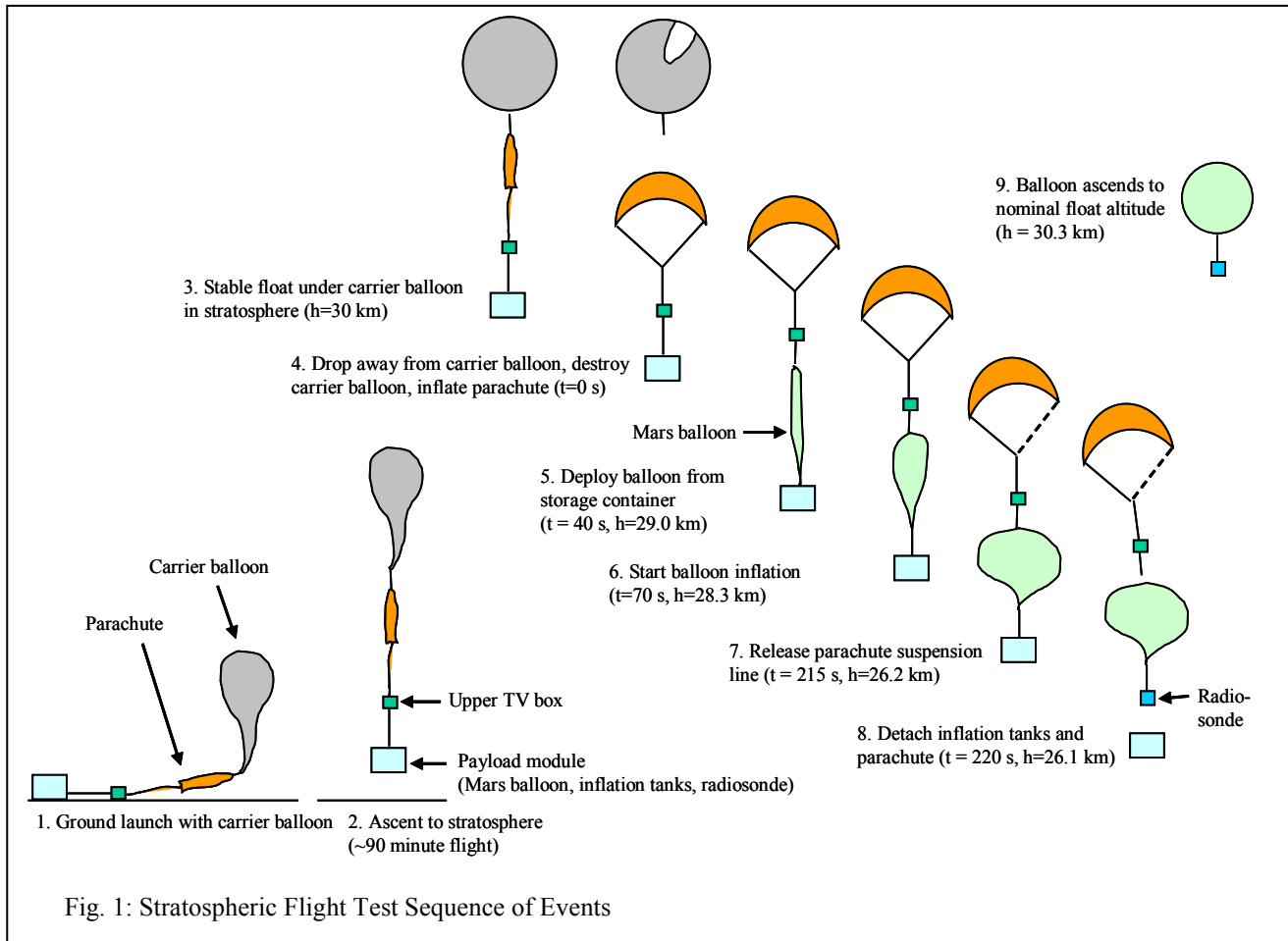


Fig. 1: Stratospheric Flight Test Sequence of Events

Each flight experiment has a number of sensors to provide data in addition to the real time video feeds from the upwards- and downwards-looking cameras. A customized Sippican Mark IIA radiosonde is attached to each payload module to provide atmospheric temperature and GPS coordinates at a 1 Hz frequency, from which pressure and altitude are accurately computed. In addition, this customized radiosonde transmits 3 more channels of data from the helium inflation system: tank pressure, tank temperature and balloon bottom fitting temperature. All of this data is collected by a Sippican W9000 ground station interfaced to a laptop computer for data display and manipulation. The radiosonde telemetry is collected on a 10 dBd Yagi antenna with a nominal range of 250 km given the 240 mW transmitter output of the Mark IIA radiosonde. Video telemetry streams are collected by a ground station antenna system consisting of a quad array of 16dBd Yagi antennas (22dBd gain total) for receiving the two color NTSC video downlinks. Flight video transmitters are 1 W into 0 dBd wheel antennas, giving a nominal video link range of approximately 300 km for snow-free video.

Each aerial deployment flight experiment is sequenced by radio commands sent by an operator on the ground through a portable transmitter unit. It provides a 45 W command radio signal sent through a 7.5 dBd Yagi uplink antenna with a nominal range of 650 km. Each command fires a pyrotechnic device on the payload that either opens a valve or cuts a rope. The command sequence for STRA-14 is listed in Table 3 and the sequences for STRA-15 is listed in Table 4. Note the use of three pyrotechnically opened valves to control the flow of helium gas into the balloon. The inflation plumbing is a simple blowdown system from 31 MPa (4500 psi) helium tanks through three parallel fixed orifices that are each paired with normally closed pyrotechnic valves that are opened in sequence. The first orifice is 0.76 mm in diameter and provides a low 4 g/s initial flow rate to create an initial gas bubble in the balloon. The gas bubble separates the balloon film sufficiently to allow the high gas flow rate to be safely injected into the balloon. The flow rate then increases to a much higher rate with valves 2 and 3, a rate selected to fill the balloon in a time period of 90 to 150 s depending on the test. Table 5 summarizes the orifice valve diameters, peak flow rates, flow durations and helium tank pressures for the three aerial deployment tests.

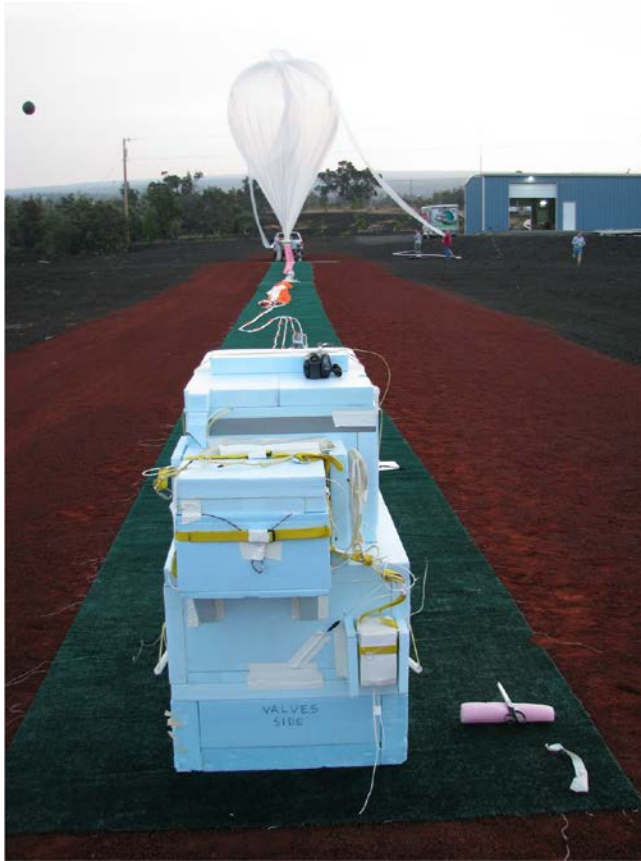


Fig. 2: Aerial Deployment Test Flight Train Prior to Launch (STRA-15).

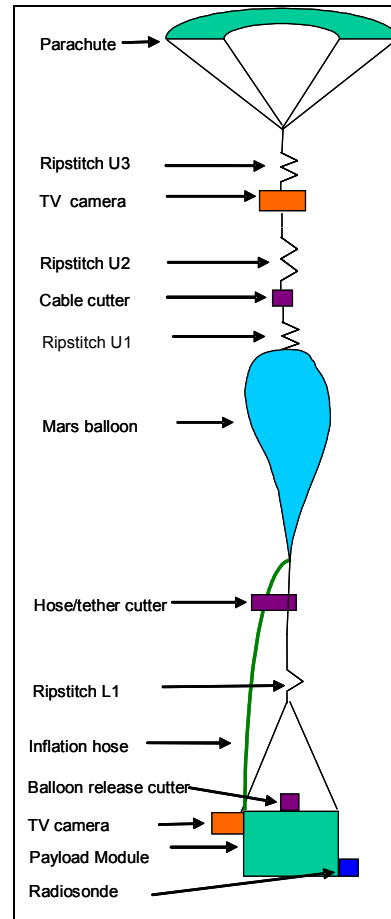


Fig. 3: Aerial Deployment Test Flight Train Schematic (Step 5 of Fig. 1.)

Table 3: STRA-14 Command Sequence

Time (m:ss)	Command
0:00	Carrier balloon separation (cable cutter)
1:00	Balloon box open (cable cutter)
1:30	Open 1 st helium valve (pyro valve)
1:40	Open 2 nd helium valve (pyro valve)
1:50	Open 3 rd helium valve (pyro valve)
2:55	Cut away parachute (cable cutter)
3:00	Cut inflation hose, drop payload module (hose cutters)

Table 4: STRA-15 Command Sequence

Time (m:ss)	Command
0:00	Carrier balloon separation (cable cutter)
0:20	Cut U1 ripstitch bypass line, U1 starts ripping to full length (cable cutter)
0:40	Balloon box open (cable cutter)
1:10	Open 1 st helium flow (pyro valve)
1:20	Open 2 nd helium valve (pyro valve)
1:50	Open 3 rd helium valve (pyro valve)
3:35	Cut parachute suspension line (cable cutter)
3:40	Detach from parachute, cut inflation hose, drop payload module (hose & cable cutters)

Table 5: Inflation System Parameters

Designation	STRA-13	STRA-14	STRA-15
Balloon Type	Sphere	Pumpkin	Sphere
Helium Mass in Storage Tanks (kg)	2.4	2.0	2.4
Helium Tank Starting Pressure (MPa)	31	31	31
Duration of Helium Inflation (s)	100	100	150
Orifice Valve #1 Diameter (mm)	0.79	0.79	0.79
Orifice Valve #2 Diameter (mm)	2.03	2.03	1.65
Orifice Valve #3 Diameter (mm)	2.54	2.54	2.54
Peak flow rate (g/s)	69	69	48

III. STRA-13 Flight Test Results

The STRA-13 sphere balloon flight occurred on the morning of June 27, 2007. Following a successful launch of the carrier balloon and flight train, a problem occurred during ascent to the stratosphere. This problem was revealed by the downward-looking video camera that showed the top of the payload module (Fig. 4). Despite being rolled up inside the payload module, the Mars balloon expanded in the low density upper atmosphere due to trapped residual air inside the balloon. The balloon expansion eventually grew to the point that it pushed up on the lid on the balloon storage box until it broke. As the flight train continued its ascent, the balloon continued to grow until it reached an approximately 1 m diameter size just prior to deployment as shown in Fig. 4. The flight video showed this bubble quickly bursting during deployment due to mechanical interference with the remnants of the balloon box lid that pushed up from below during opening. This failure ended the experiment and no other useful data was collected during this flight test.

Post-flight analysis suggested a combination of factors that contributed to the residual gas problem and consequent structural failure. No previous flight test had shown this kind of behavior in which the balloon expanded and broke the payload module lid from below. However, some minor deflections of the balloon box lid could be seen in old flight videos, which is suggestive of a less serious residual gas problem. For STRA-13 and previous flight tests, the top of the Mars balloon was not capped so as to provide a direct vent path for residual gas to escape out of the top of the balloon during ascent to the stratosphere. It appears that this venting was greatly hindered on STRA-13 by two subtle changes from previous flights. The first change was that the internal porous fabric inflation tube was extended all the way to the top fitting, in contrast to previous years for which the tube was connected with a short length of fabric ribbon leaving the top fitting uncovered. This tube is intended to serve as an additional diffuser element that prevents direct impingement of high speed helium gas onto the balloon envelope during inflation. The second change was that the STRA-13 sphere balloon was packed more efficiently than any previous test in the sense that it was very tight and occupied a smaller volume. The combination of these two changes served to effectively block the vent path for residual gas to escape through the top fitting, with the porous inflation tube

adding a barrier not previously there, and the tight packing serving to compress it and largely choke off the flow path.

A post-flight volumetric analysis revealed that approximately one-third of the residual gas was contributed from the inflation hose connecting the orifice valves and the balloon, and two-thirds was contributed from gas inside the balloon itself. One implication of this is that efforts to avoid the problem by completely evacuating the gas from inside the balloon will not work unless it is coupled with an evacuation of the tubing as well.



Fig. 4: STRA-13 extruded balloon problem.

IV. STRA-14 Flight Test Results

The STRA-14 pumpkin balloon flight occurred on the morning of June 30, 2007. This flight test occurred only three days after the STRA-13 failure and prompted two modifications to the test approach so as to avoid the same residual gas problem. The first change was to drill a small 0.5 mm diameter hole into the flex hose to provide a direct vent path for residual gas in the hose itself. This hole was small enough that it would leak only a tiny fraction ($\ll 1\%$) of the helium input gas during inflation. The second change was to place the pumpkin balloon into a vacuum chamber for a couple of hours and attempt to remove as much air as possible from inside the balloon. In addition, the balloon top fitting design was re-evaluated to assess whether the same vent path blockage problem could be experienced. The conclusion was that this blockage would not occur because of the much looser accordion folding of the pumpkin balloon compared to the tight rolling of the STRA-13 sphere and the fact that the internal inflation tube did not cover the top fitting into the pumpkin balloon. As it turned out, the STRA-14 flight did not suffer from any residual gas problems. Launch was nominal and the desired stratospheric flight altitude of 31 km was attained an hour and a half after launch.

The STRA-14 aerial deployment and inflation experiment experienced a combination of success and failure. The pumpkin balloon deployed successfully with no apparent structural damage as seen in the video. However, during the deployment, the downward-looking video camera failed. Post-flight data analysis was not conclusive, but suggested that the deployment shock force mechanically broke the adhesive joint that connected the camera to its support structure. The consequence of this failure was that only upward-looking video was obtained for the bulk of the deployment sequence and all of the inflation sequence.

Figure 5 shows a set of six images captured from the upward-looking video during the pumpkin balloon inflation process and subsequent parachute detachment. The full sequence was successfully executed with all pyrotechnic devices functioning properly and all separation events occurring. Helium tank pressure measurements confirmed that the helium gas was injected into the balloon in the planned 90 s period. However, the video evidence clearly shows that the balloon envelope was damaged in multiple places during the inflation. The first visible holes in the envelope are seen shortly after the peak helium flow rate time of 20 s after inflation start (Fig. 5c). The video shows that the internal porous inflation hose was thrashing about wildly during this time, undergoing whip-like motion around the time of peak inflation rate. Although the video evidence is not conclusive, the post-flight conclusion by the team was that the inflation hose smashed against the balloon envelope multiple times and broke the polyethylene film in multiple gores. This was an ironic result given the fact that the porous inflation tube's function was to protect the balloon envelope from direct helium impingement. Despite this damage, the pumpkin balloon almost completely fills out by the end of inflation, just like an undamaged balloon would (Fig. 5d). The experiment was sequenced through to completion with both parachute and payload module separation successfully occurring (Figs 5e and 5f). Unfortunately, the radiosonde that should have flown with and tracked the separated pumpkin balloon broke away from the balloon during the payload module separation event and so no data was obtained on the float behavior. Fig. 5f does show lateral separation of the parachute and balloon, indicating that the strategy of making the parachute glide just prior to separation worked to prevent it from falling on top of the balloon.



Fig. 5a: Pumpkin balloon and cross parachute just prior to inflation ($t = 0$ s). White flex hose visible at lower left.

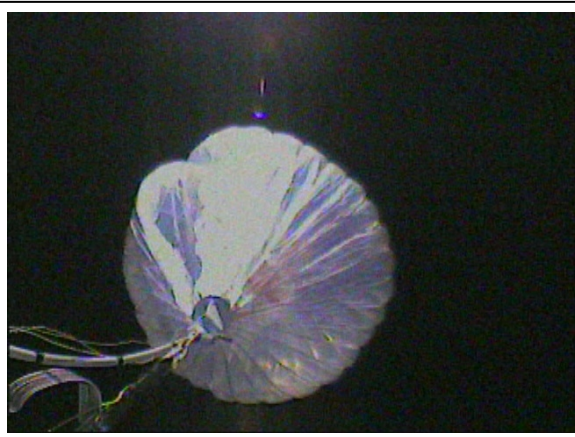


Fig. 5b: Early inflation is fine at $t = 10$ s, just prior to opening of the second orifice valve that initiates a high flow rate.



Fig. 5c: Tear/hole obvious at $t = 22.5$ s, just after third orifice valve opened.

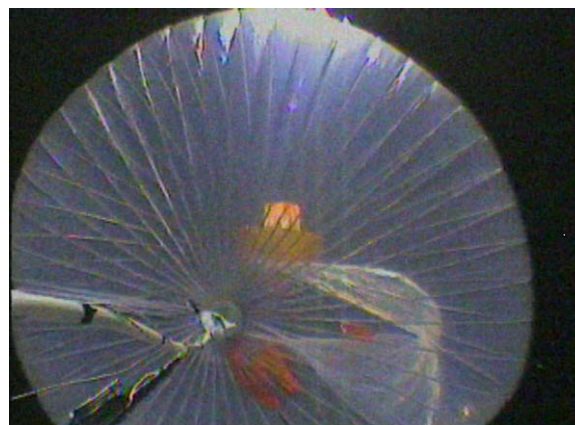


Fig. 5d: Balloon fills up despite tears ($t = 42.2$ s). Note orange cross parachute visible through balloon and orange inflation tube near bottom.



Fig. 5e: 1 sec after payload module and parachute separation ($t = 91.0$ s)



Fig. 5f: Balloon and cross parachute laterally displaced ($t = 93.9$ s)

The primary conclusion drawn from the STRA-14 flight is that the combination of a peak helium flow rate of 69 g/s and the use of a long, thin porous internal inflation tube results in violent, whip-like motion of the tube that impacts and damages the balloon. This was seen as a relatively tractable problem and design changes were made to the subsequent flight test, STRA-15, consisting of a new inflation tube design and a reduction in peak flow rate from 69 to 48 g/s. Although there were problems with the downwards-looking video camera and the radiosonde, all other core aspects of the Mars pumpkin balloon aerial deployment test were successful. In particular, the aeroelastic behavior of the partially inflated balloon during the parachute descent was quite benign, providing further evidence that very low dynamic pressures of approximately 5 Pa yield favorable conditions for Mars balloon aerial inflation. This benign behavior also allows for the use of lower helium flow rates that require longer inflation periods while descending under the parachute.

V. STRA-15 Flight Test Results

The STRA-15 sphere balloon flight occurred on the morning of June 14, 2008. Following a nominal launch, the carrier balloon and flight train successfully ascended to the planned float altitude of 30 km. The residual gas problem experienced on flight STRA-13 was not seen here. Much like the STRA-14 pumpkin flight of the prior year, this resulted from providing clear vent paths for residual gas to get out of both the top and the bottom of the balloon during ascent. An open valve was placed at the top of the balloon and it remained open during the entire ascent to the stratosphere. It was mechanically rigged such that the balloon deployment transient shock force would close the valve prevent any helium gas leak gas during inflation. A custom-designed check valve was located at the bottom of the balloon so that it could vent gas during ascent to the stratosphere, but would automatically close and prevent helium gas from exiting during balloon inflation. This check valve was oriented to allow the normal flow of helium gas from the inflation tanks into the balloon. The combination of closable valve at the top and check valve at the bottom provided the first implemented design that satisfied the twin requirements of gas venting during ascent with a gas-tight seal during inflation and subsequent float of the Mars balloon.

The other major design change from the 2007 flight experiments was for the porous inflation tube. Instead of a long thin tube employed on every other Mars balloon stratospheric flight test, a new design was used that had the shape of a cone with the fat end on the bottom at the junction with the balloon end fitting (Fig. 6.) This actual flight tube was tested under full flow conditions (50 g/s) in a vacuum chamber to confirm absence of the whip-like motions seen in STRA-14. The new design behaved very stably in these laboratory tests while fulfilling the original design intent of diffusing the helium gas flow and preventing the direct impingement of a high speed helium jet on the balloon envelope. After laboratory testing, this inflation tube was used to build the STRA-15 Mars flight balloon.

Unfortunately, the STRA-15 spherical balloon catastrophically broke during the aerial deployment stage of the flight test and so the inflation step was not reached and no performance data for it was obtained. The balloon structural failure consisted of a complete break of the balloon at the junction of the end cap reinforcement with the main balloon gores. Fig. 7 shows a downwards-looking view of the Mars balloon and flight train at the moment of failure. The broken edge of the balloon is clearly visible. In subsequent video frames one can see the break propagate around the rest of the end cap, leaving the balloon in two parts with the bottom receding from view, still attached to the payload module.

This kind of balloon structural failure during deployment had not been seen since the STRA-5 test of a 10 m sphere balloon in 2001. Since that time, the new ripstitch design model and reinforced end cap construction of the balloon had apparently solved the problem of excessive balloon stress during the transient deployment shock loads. Post-flight data analysis of STRA-15 did not pinpoint the cause of this failure, but there are a few suggestive clues. The first is that the failure occurred on the larger 12 m diameter sphere balloon but not on the previous three 10 m aerial deployments. The larger size will produce a larger deployment shock load since the balloon



Fig. 6: STRA-15 Inflation Tube during laboratory flow test at low pressure.

falls further during the gravity drop deployment and converts more gravitational potential energy into kinetic energy and hence strain energy when the balloon reaches full extension.

The second clue can be seen in Fig. 7. The Mars balloon is displaced laterally to the upper left side to form an arc-like shape. This lateral displacement occurred despite no known lateral force acting on the system. Earlier frames from the video show a straight and vertical flight train with no lateral motion or apparent lateral wind loading. This kind of lateral movement must correspond to unequal stress loading of the balloon gores, with the gores on the outside of the arc gores loaded and the gores on the inside of the arc basically unloaded. The photograph clearly shows that the outside edge is where the balloon broke. Therefore, this suggests that the lateral motion and resultant balloon shape caused the transient shock loads to be borne by only a subset of the balloon gores, which became overstressed and failed. This large lateral motion was not observed in prior stratospheric flight tests, although much lesser deviations from vertical can be seen in the old flight videos.



Fig. 7: STRA-15 sphere balloon at the moment of structural failure. Note broken circular edge of balloon highlighted in red.

The cause for the lateral motion is not known. The fact that the balloon can deviate from a strictly vertical line indicates that the top of the payload module and the bottom of the parachute must move towards each other and reduce their separation distance, otherwise the Mars balloon could not take on the arc shape seen in Fig. 7. It is plausible that there is a recoil in the balloon as it reaches its maximum deployed length, a recoil that pulls down on the parachute and slightly decreases the separation distance to the payload module. A natural consequence of this decreased separation distance will be for the balloon to laterally displace in an arc-like shape as seen. This is perhaps analogous to a guitar string that is quickly pulled taut and then vibrates perpendicular to the direction of the string. A review of upward-looking flight video from the prior STRA-11 sphere balloon test is consistent with this transient parachute pull-down hypothesis. However, the upward-looking video camera on STRA-15 failed during ascent and corroboration of the parachute motion could not be assessed for this flight.

Whatever the cause, the ability of this system to experience large lateral movements that put high stresses on only a subset of balloon gores is a very troubling result, one that calls into question the viability of the gravity drop deployment technique. There is not sufficient design flexibility to engineer the sphere balloon in such a way that it can load only some of its gores (perhaps as little as a half) in this high load process and still tolerate the resulting material stresses. There is no video evidence that the ripstitch did any ripping in STRA-15, suggesting that the use of ripstitch cannot mitigate this particular effect. It appears likely that a robust solution will require an alternate approach based on reduction of the speed of the balloon deployment, with an attendant reduction in the stresses experienced by the balloon when it reaches its full deployed length at the end of the process. Devices like the descent rate limiter (DRL) used as part of the Mars Pathfinder and Mars Exploration Rover missions landing sequence could be applicable here to limit the speed with which the balloon deploys and thereby bring the balloon material stresses well below the tolerable limit.

The balloon structural failure essentially ended the STRA-15 experiment and no other useful data was acquired for the inflation and separation processes.

VI. GRND-1 Flight Test Results

A key premise of the JPL-Wallops-NSC Mars balloon technology program is that once the Mars balloon gets through the aerial deployment and inflation process, it floats in such a benign environment that stable, long-lived flights are likely. The ground-launched flight experiment, GRND-1, was conducted to gather evidence in support of this premise. The need is to get the Mars balloon floating under Mars-like conditions without suffering any damage prior to getting there. A direct ground launch of the Mars balloon will avoid the high stresses associated with the

aerial deployment process by taking advantage of a ground crew that can carefully handle the balloon in such a way as to maximize its chances of starting in a damage-free condition. Just such an experiment was conducted on the morning of June 11, 2008. The balloon was a copy of the 12 m diameter sphere flown in STRA-15. It carried a payload that included an upwards-looking video camera and a Sippican Mark II radiosonde that provided tracking via an onboard GPS receiver.

The ground-launched flight test was very successful. The Mars balloon safely ascended to a 30,275 m altitude just before local noon and maintained this altitude for the next 8.5 hours with a variation of only ± 75 m. Fig. 8 shows the Mars balloon shortly after launch, Fig. 9 shows the balloon soon after reaching its stratospheric float altitude, and Fig. 10 shows the altitude plot for the flight. Note that the balloon was stable in altitude despite going from the full noontime sun to sunset. Maintaining altitude stability under this full range of solar heating is highly indicative of a leak-free balloon. The helium fill of this balloon was 2.509 kg, designed to provide a surface free lift of 14% and a maximum superpressure of 260 Pa under the noontime sun. This compares to an expected burst superpressure of 820 Pa based on membrane theory for a perfect sphere. This gives a safety factor of 3.1, comparable to what is expected for an actual flight mission at Mars. The corresponding nighttime superpressure is 180 Pa, or an excess of 350 g of helium compared to neutral buoyancy. Note that the batteries on the telemetry system failed after 8.5 hours of flight at altitude, after which balloon tracking was lost. The balloon was 440 km from the launch site at that time. It is unknown how much longer the balloon continued to fly.

In summary, the Mars spherical balloon performed very well under Mars-like conditions in the Earth's stratosphere in this test. This gives confidence that the balloon will function equally well at Mars and provide a long flight lifetime assuming it can survive the aerial deployment and inflation process without damage.



Fig. 8: Mars balloon shortly after ground launch for test GRND-1.

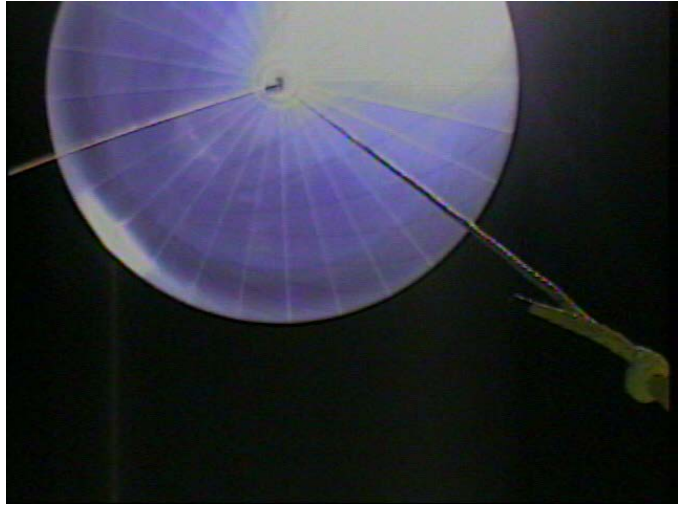


Fig. 9: GRND-1 balloon shortly after reaching the stable float altitude of 30.275 km.

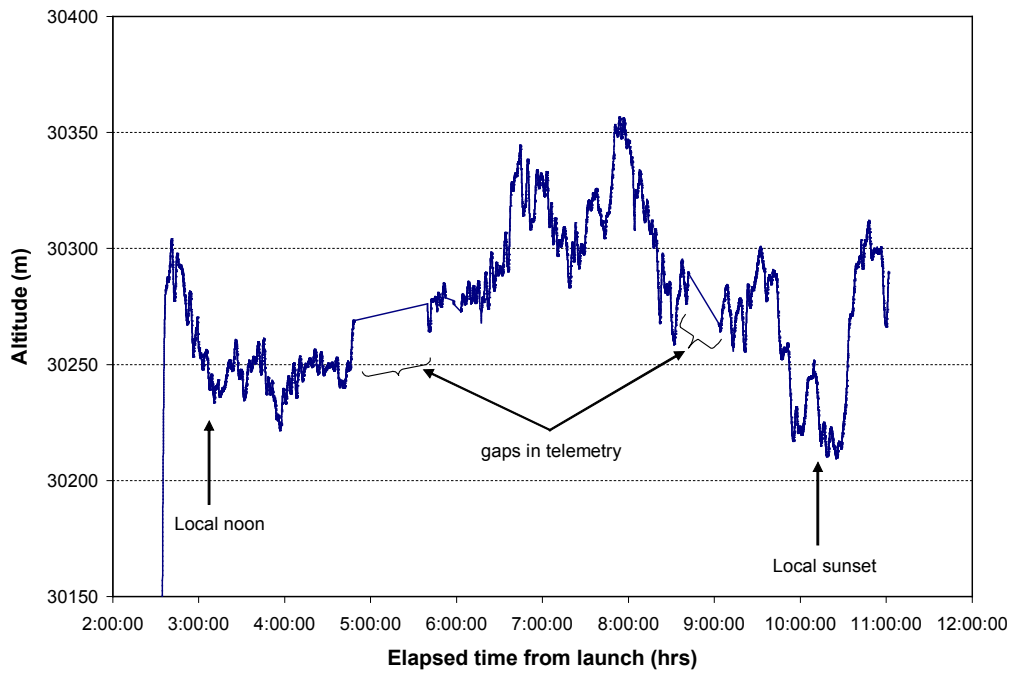


Fig. 8: Altitude Plot for GRND-1.

VII. Conclusions

This paper has described a set of four stratospheric flight experiments with prototype Mars balloons. Three of the experiments were aerial deployment and inflation tests designed to validate an end-to-end approach from packaged balloon to floating balloon. Two tests involving 12 m diameter sphere balloons failed, one from residual gas that extruded the balloon out of its storage container, the other during a normal gravity drop deployment that somehow overloaded the balloon and caused immediate and catastrophic structural failure. It is likely that future sphere balloon deployments will use a different strategy than the gravity drop deployment in which some form of speed controlled deployment of the balloon is used to greatly minimize the transient stresses experienced by the balloon material. A third test of a 660 m³ pumpkin balloon successfully deployed, inflated and separated the balloon, but the inflation process caused damage to the Mars balloon. Telemetry failures prevented knowledge of how well that balloon flew after separation. The fourth and final test was of a ground-launched 12 m diameter sphere balloon. This balloon was highly successful, reaching a float altitude of 30,275 m and stably floating there for 8.5 hours with an altitude variation of only ± 75 m. The ability of this sphere balloon to maintain altitude over this period that spanned from noontime to sunset is a strong indicator that the balloon was leak free and possessed the required structural strength and superpressure margins to support long duration flights at Mars.

Acknowledgments

The authors would like to thank the following people for their assistance in the performance of this project: Bob Blackington, Wert Russert and Kevin Carlson of Near Space Corporation, and Alex Mora of JPL. The research described in this paper was led by the Jet Propulsion Laboratory, California Institute of Technology, under a contract with the National Aeronautics and Space Administration that was administered through the Mars Technology and Innovative Partnership Programs.

References

- ¹ Kerzhanovich, V. V., Cutts, J. A., Cooper, H. W., Hall, J. L., McDonald, B. A., Pauken, M. T., White, C. V., Yavrouian, A. H., Castano, A., Cathey, H. M., Fairbrother, D. A., Smith, I. S., Shreves, C. M., Lachenmeier, T., Rainwater, E., Smith, M., "Breakthrough in Mars balloon technology", *Advances in Space Research*, Vol. 33, No. 10, pp. 1836-1841, 2004.
- ² Jeffery L. Hall, Michael T. Pauken, Viktor V. Kerzhanovich, Gerald J. Walsh, Debora Fairbrother, Chris Shreves and Tim Lachenmeier (2007). "Flight Test Results for Aerially Deployed Mars Balloons", AIAA Paper 2007-2626, presented at the AIAA Balloon Systems Conference, Williamsburg, VA, 21-24 May, 2007.